

# A Realistic Protocol for Evaluation of Weakly Supervised Object Localization

Shakeeb Murtaza, Soufiane Belharbi, Marco Pedersoli, Eric Granger

LIVIA, Dept. of Systems Engineering, ETS Montreal, Canada

shakeeb.murtaza.1@ens.etsmtl.ca

## ABSTRACT

*Weakly Supervised Object Localization (WSOL) allows training deep learning models for classification and localization (LOC) using only global class-level labels. The absence of bounding box (bbox) supervision during training raises challenges in the literature for hyper-parameter tuning, model selection, and evaluation. WSOL methods rely on a validation set with bbox annotations for model selection, and a test set with bbox annotations for threshold estimation for producing bboxes from localization maps. This approach, however, is not aligned with the WSOL setting as these annotations are typically unavailable in real-world scenarios. Our initial empirical analysis shows a significant decline in LOC performance when model selection and threshold estimation rely solely on class labels and the image itself, respectively, compared to using manual bbox annotations. This highlights the importance of incorporating bbox labels for optimal model performance. In this paper, a new **WSOL evaluation protocol** is proposed that provides LOC information without the need for manual bbox annotations. In particular, we generated noisy pseudo-boxes from a pretrained off-the-shelf region proposal method such as Selective Search, CLIP, and RPN for model selection. These bboxes are also employed to estimate the threshold from LOC maps, circumventing the need for test-set bbox annotations. Our experiments<sup>1</sup> with several WSOL methods on ILSVRC and CUB datasets show that using the proposed pseudo-bboxes for validation facilitates the model selection and threshold estimation, with LOC performance comparable to those selected using GT bboxes on the validation set and threshold estimation on the test set. It also outperforms models selected using class-level labels, and then dynamically thresholded based solely on LOC maps.*

## 1 Introduction

Methods for WSOL provide efficient learning strategies [1–3] to mitigate the cost of annotating datasets with bboxes. Given only coarse image-class labels, a deep learning model can be trained to perform image classification (CL) tasks while yielding the spatial im-

age region of the object (localization). Class-Activation Mapping (CAM) [4, 5] is the dominant WSOL approach that builds a spatial heatmap to localize an object.

Despite its popularity, WSOL still faces several challenges, in particular with its evaluation protocol [4]. We argue that the common protocol presently used in the literature may not be reliable for real-world applications limiting WSOL benefits. WSOL methods should only require image-class labels for supervision. During training (with held-out validation sets), the model should not have access to data with manual localization (LOC) supervision, i.e., ground truth (GT)

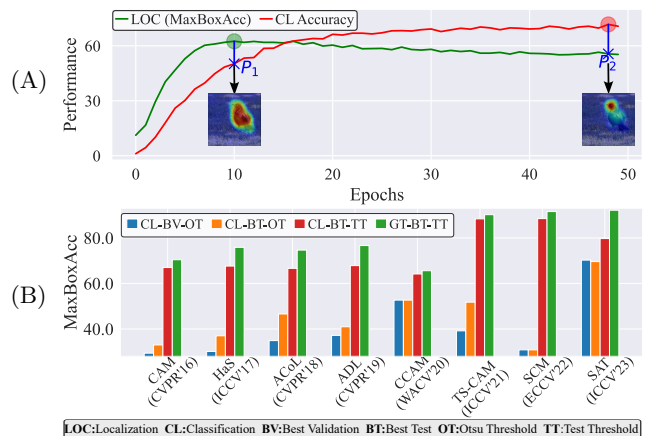


Figure 1: (A) Example of LOC (**MaxBoxAcc**) and **CL** accuracy w.r.t the number of epochs on the CUB validation set in a WSOL setting, where only image-class labels are used to train the model. These curves show that LOC and CL tasks are loosely correlated where convergence is reached at different training epochs. Typically, high LOC performance is achieved early in the training, followed by degradation. However, the classifier takes a longer time to converge. Selecting the best model for LOC may need a LOC annotation in the validation set. (B) Significant bias arises when using GT bounding boxes and test set thresholds, leading to overestimated LOC accuracy, as bbox annotations are typically absent in real-world scenarios. *In a realistic WSOL scenario (CL-BV-OT), where model selection is based on CL accuracy and OT over the validation set, performance declines considerably.*

<sup>1</sup>Our code and the generated pseudo-boxes are available at [github.com/shakeebmurtaza/wsol\\_model\\_selection](https://github.com/shakeebmurtaza/wsol_model_selection).

bounding box (bbox) annotations. Model selection and hyper-parameter search are therefore very challenging (Fig.1A). Early works observed the test performance for hyper-parameter selection leading to an overestimation of model performance [6–8]<sup>2</sup>. As illustrated in Fig.1B, the test-set LOC performance of these methods may decline in real-world scenarios, where only image-class labels are available.

Choe et al.[4] proposed an improved evaluation protocol to address some of the above limitations. To perform model selection, they propose using a held-out validation set with full manual annotations (class labels and bboxes). Although this protocol allows us to avoid using the test set and to perform unbiased modal evaluations, it is somewhat unrealistic since annotated bboxes are not available in practice. Having access to such manual LOC supervision during training goes against the WSOL setting, and can overestimate model performance (Fig.1B). Moreover, the same authors [4] have shown that a model directly trained on those annotated images would provide higher LOC accuracy than any weakly supervised approach. Although authors annotated a limited number of images per class to create a held-out validation set, the total cost of annotation adds up with the number of classes. For instance, they annotated 10 images/class for the ILSVRC dataset, which amounts to a total of 10,000 images. Given the cost, these fully annotated images can, for example, be directly used to fit the model weights in a semi-supervised learning (SSL) setting rather than being used for model selection in a WSOL setting.

Another unrealistic practice prevalent in the literature is the use of GT bboxes from the test set to estimate the threshold for binarizing the LOC map to generate bboxes [4]. However, this practice leads to an overestimation of model performance (LOC accuracy) because bbox annotations are typically absent in real-world scenarios, making it impossible to estimate the threshold during inference. Models selected using GT bboxes and test set thresholds may exhibit significantly higher LOC accuracy than models selected based on CL accuracy and thresholds automatically estimated using the Otsu thresholding (OT) algorithm, for example, as one would do when bbox annotations are unavailable on the validation. An example of the inflated performance resulting from using the test set for model selection and threshold estimation is illustrated in Fig.1B, where the LOC accu-

racy is reported for various WSOL methods on the CUB test set using two model selection criteria: CL and LOC accuracy. Additionally, the results of different thresholding methods are reported for LOC maps used to generate bboxes. Additionally, we presented the test LOC accuracy when the model was selected with the best CL accuracy on the validation or test set, and when automatic thresholding algorithm (OT) was used for producing bboxes. In a more realistic evaluation protocol, where model selection is based on CL accuracy and the OT on the validation set (blue bar Fig.1B), a noticeable decrease in performance is observed. This assessment highlights the necessity for unbiased thresholding and model selection to evaluate the real-world capabilities WSOL of methods.

This paper provides a realistic evaluation protocol for WSOL that can be applied in real-world scenarios. Instead of assuming that manual bbox annotations are available for the validation set, we propose estimating pseudo-bbox (Fig.3). To do so, we leverage an off-the-shelf pretrained model that can generate region-of-interest (ROI) proposals [9] such as Contrastive Language–Image Pre-training (CLIP) [10] method. This model is pretrained on generic datasets requiring less supervision, such as image-class labels. We also consider Selective Search (SS) [11], an unsupervised method that does not require training, and Region Proposal Network (RPN) [12] are trained on large datasets with class-agnostic bboxes. They can generate multiple bboxes with objectness scores to rank them. We aim to explore the impact of using these different supervisions for pretrained proposal generators. Given a set of proposed bboxes for an image, and using pointing game analysis [13] and image-class label, the most discriminative boxes are selected and ranked using classifier response to produce the final bbox. This approach allows us to create pseudo-annotated bboxes for the held-out validation set, and therefore, avoid manual annotation, leading to more realistic model selection in WSOL. Despite their lower accuracy, these pseudo-bboxes can effectively select models and enable the estimation of thresholds using the validation set for generating bboxes from LOC maps in the test set.

To address the biased estimation obtained with current approaches, a threshold is estimated using the validation-set pseudo-boxes and subsequently applied to the test set to convert LOC maps into bboxes. Estimating the threshold from the validation set enables WSOL methods to achieve realistic and competitive performance in real-world scenarios. This avoids estimating the threshold from the test set, which leads to an over-

<sup>2</sup>Refer to the official implementation [6–8] that is publicly available. Unfortunately, even recent works after [4] still use the test set as a held-out validation set [3] as shown in their public code. This practice potentially biases the selection process in favor of LOC performance.

estimation of performance, and using OT which leads to low performance (see Fig.1B).

**Our main contributions are summarized as follows.**

(1) An initial experimental analysis of state-of-the-art WSOL methods on the CUB and ILSVRC datasets showing the impact of supervision in the held-out validation set on test performance. Results indicate that utilizing only image-class labels for validation leads to poor test-set LOC accuracy, highlighting the importance of using LOC cues for model selection. Conversely, manually annotated bboxes for validation improve the estimation of LOC accuracy, leading to an overestimated and unrealistic performance evaluation. Further experiments evaluating the use of less precise pseudo-bbox supervision in the validation set indicate that noisy bboxes can still effectively guide model selection.

(2) A realistic evaluation protocol is proposed for WSOL; First, we propose to estimate pseudo-bboxes without manual intervention and use only image-class labels to generate annotations for a held-out validation set. Given different application scenarios, we explored three different bbox generation strategies based on off-the-shelf models: SS [11], RPN [12], and CLIP [10]. Secondly, these pseudo-bboxes generated for the validation set allow for estimation of the threshold, which can be subsequently applied to test images for producing bboxes on the LOC maps.

(3) An extensive set of experiments was conducted with prominent WSOL methods using our new experimental protocol on the CUB and ILSVRC datasets for model selection and threshold estimation to convert localization maps into bboxes. The results demonstrate that models selected and thresholds estimated using pseudo-bboxes achieve a level of accuracy comparable with the unrealistic selection protocol, wherein bboxes are utilized for model selection over the validation set and threshold estimation using the test set. Moreover, utilizing one threshold estimated using pseudo-boxes reduced the number of thresholds required to search for the optimal value from 1,000 to 1.

## 2 Related Work

In standard supervised learning, hyper-parameter and model selection typically rely on a fully annotated validation set. Methods like early stopping leverage this set for realistic estimation of model performance on unseen test data [14–16] since the three sets (train, val and test) employ the same supervisory signal and perform the same task. The rest of this section reviews model selection protocols in different settings, highlighting is-

ues in model selection and hyper-parameter search. It also discusses early stopping without a validation set and concludes with model selection in WSOL.

(a) **Protocols with limited supervision.** Beyond the fully supervised setting, other learning settings have been derived with their protocol. This typically concerns learning with less annotated data [17, 18]. This may affect the availability of annotations over the held-out set used for model selection and hyper-parameter search. Despite the efforts of the community to design standardized protocols, unrealistic practices may emerge. Different attempts have been made to ensure that such protocols are realistic to benefit from the unbiased application in real-world scenarios.

In the SSL setting, researchers have investigated whether exiting works can perform well on realistic benchmarks compared to standard benchmarks used by the community [19, 20]. The authors argue that standard SSL benchmarks fail to reflect real-world challenges such as sensitivity to unlabeled data size, distribution shifts, class imbalance, and novel classes, and reserving some labeled samples as a held-out validation set reduces the training set size.

Unsupervised domain adaptation (UDA) is another learning setting with less annotation that raises several questions about how realistic is the protocol. UDA involves adapting a source model on labeled source data and unlabeled target data. Model selection and hyper-parameter search are challenging, with recent works improving evaluation protocols [21–26]. For instance, Ericsson et al. [22] show that using an annotated target set for hyper-parameter search leads to largely overestimated and unrealistic performance. They proposed using source data, evaluating another UDA model such as InfoMax [27], or a labeled held-out target set. Yang et al. [25] introduced the Transfer Score for UDA model evaluation for hyper-parameter search and early stopping. The protocol issue is much more severe in the case of source-free UDA [28] where the user cannot access the source data.

Self-supervised [29], unsupervised learning [30, 31], and data generation [32] also face model selection and hyper-parameter search difficulties due to limited supervision. For instance, in image generation, quantitative measures [33–35] may not fully capture how realistic a generated image is, necessitating visual inspections that affect reproducibility and real-world applicability.

The aforementioned works show that the evaluation protocol is an issue for many settings. In this work, we focus on realistic WSOL evaluation protocols, in particular model selection for hyperparameter optimization

and producing threshold for test set to produce bboxes from localization maps.

**(b) Early stopping without validation set.** Some works have explored early stopping without a validation set, crucial when data is limited. Large held-out validation sets improve generalization estimates but reduce training data size at the cost of significantly reducing the data available for the training set. Mahsereci et al.[36] proposed a criterion using gradient statistics over the training set, effective in classification and regression tasks. Duvenaud et al.[37] used weight statistics, monitoring the entropy change in network parameters as an indicator of generalization. Yuan et al.[38] introduced *Label Wave*, tracking model prediction changes on noisy training labels to prevent overfitting. Li et al.[39] suggested using augmented training data instead of a real validation set to reduce computational costs. While these works aim to halt the training of the entire model, Bonet et al.[40] per-class channel early stopping for CNNs without validation sets, leveraging DeepNNK[41], a non-negative kernel regression. Note that in these works, the training and test task is the same. In WSOL, however, the model is trained for the CL task but it is evaluated on the LOC task.

**(c) Protocols for WSOL.** Before the work of Choe et al. [4], bbox annotations were not considered to create the held-out validation set. Therefore, practitioners may unintentionally inspect the test LOC performance, leading to unrealistic WSOL [6–8]. To alleviate this, Choe et al. [4] investigated several aspects of WSOL protocol. They mainly showed that state-of-art methods (at that time) do not improve accuracy beyond that of the baseline CAM method [42] after searching for the optimal decision threshold. They proposed a concise WSOL evaluation protocol, including new metrics and a held-out validation with bboxes. Although their work largely improved the WSOL protocol, it is somewhat unrealistic since manually-labelled bboxes are not available in real-world applications of the WSOL setting. Strong supervision is used to select a model, which implicitly helps to select a model with the best LOC performance which can contribute to overestimating LOC accuracy on the test set. In addition, it has been reported [4] that using manually annotated bboxes for model training on the held-out validation set, rather than image-class labels on the training set, can outperform baseline WSOL methods. Furthermore, Choe et al. [4] also employ the test set for estimating the threshold needed to convert the localization map to bboxes, rendering WSOL setting unrealistic.

Although more realistic protocols have been developed for other learning settings like SSL and UDA, WSOL

represents a challenging setting because of the different tasks (CL and LOC) performed with the same model during training vs testing. The supervision available during training allows us to select models for the CL task. At test time, the model is evaluated additionally over LOC. The disconnection between available annotation at training time, and the required task at test time creates a challenging situation for model selection. Furthermore, §3 provides a more realistic evaluation protocol within the WSOL framework.

### 3 A Realistic Protocol for Model Evaluation

In this section, we propose an improved protocol for evaluating WSOL methods. We first show that LOC accuracy can be overestimated when using manual bbox supervision for the held-out validation set. To address this, we propose automatically generating pseudo-bboxes for the validation set using only image-class supervision, eliminating the need for manual annotation. It involves generating pseudo-bboxes for the validation set using existing off-the-shelf ROI proposal generators and utilizing these pseudo-bboxes to estimate a threshold, which is then applied to localization maps in the test set for producing bboxes, providing a more systematic and realistic evaluation protocol.

#### 3.1 Model Selection

Consider a WSOL training set  $\mathcal{D}_{train} = \{(x_i, y_i, \cdot)\}$  composed of samples with  $x_i$  the input image,  $y_i$  its image-class label, and  $\cdot$  is its missing bbox supervision. Let us define  $\mathcal{D}_{val} = \{(x_i, y_i, \cdot)\}_{i=1}^N$ <sup>3</sup>, and  $\mathcal{D}_{test} = \{(x_i, y_i, o(x_i))\}$  as the held-out validation and test sets, respectively, where  $o(x_i)$  is the oracle manual bbox annotation for the sample  $x_i$ . In the WSOL setting, bbox supervision is unavailable for any dataset. However, in a laboratory, the test set contains them to evaluate LOC performance of a model.

The WSOL setting involves training a model  $f(\cdot; \theta)$  with parameters  $\theta$  to correctly classify an input image while yielding LOC boxes. Training is performed on  $\mathcal{D}_{train}$  that lacks LOC supervision. In this paper, we introduce a pseudo-annotator  $\hat{o}$  that automatically annotates an image with pseudo-bboxes (without human intervention) and only requires the image-class labels.  $\hat{o}$  yields noisy bboxes, providing LOC pseudo-bbox annotations  $\hat{o}(x_i)$  that are less accurate than oracle bbox annotations  $o(x_i)$ . Moreover, we redefine the validation

<sup>3</sup>In Choe et al. [4] the validation set contain  $o(x_i)$ .

set  $\mathcal{D}_{val}$  to incorporate pseudo-bboxes  $\hat{o}(x_i)$ , yielding  $\mathcal{D}_{val} = \{(x_i, y_i, \hat{o}(x_i))\}_{i=1}^N$ .

Let  $f(x; \theta)$  be the model’s CL prediction, while  $f(x; \theta)^b$  is the predicted bbox for image  $x$ . We denote by  $\ell(\cdot, \cdot)$  a LOC similarity measure between two bboxes. Following Choe et al. [4],  $\ell(\cdot, \cdot)$  is commonly **MaxBoxAcc** or simply the Intersection-Over-Union (IoU) measure. Let us define a hypothetical ideal scenario where one can have access to the oracle for fully annotated bboxes  $o(x_i)$  in the validation set  $\mathcal{D}_{val}$  allowing, for instance, to perform early stopping and threshold selection. Therefore, we can define the average LOC performance of the model  $f$  with a specific parameter value of  $\theta$  over this validation set as,

$$\mathcal{M}(\theta, \mathcal{D}_{val})_o = \frac{1}{N} \sum_i^N \ell(f(x_i; \theta)^b, o(x_i)). \quad (1)$$

Similarly, the same measure over  $\mathcal{D}_{val}$  can be defined using our pseudo-annotator  $\hat{o}$  as,

$$\mathcal{M}(\theta, \mathcal{D}_{val})_{\hat{o}} = \frac{1}{N} \sum_i^N \ell(f(x_i; \theta)^b, \hat{o}(x_i)). \quad (2)$$

Eqs. 1 and 2 provide an assessment of the model LOC accuracy over a held-out  $\mathcal{D}_{val}$ . Eq.1 is accurate, while Eq.2 accounts for errors due to inaccurate LOC annotation. Since practitioners do not have access to the oracle bboxes  $o(x_i)$ , the measure  $\mathcal{M}(\theta, \mathcal{D}_{val})_o$  is not realistic. When one has access to oracle  $o(x_i)$  bboxes for training, it is better to perform SSL to directly fit the model weights instead of WSOL [4]. However, one can still assess  $\mathcal{M}(\theta, \mathcal{D}_{val})_{\hat{o}}$  for an approximate but realistic estimation of the model’s LOC accuracy. The latter measure provides a realistic assessment of LOC accuracy for WSOL. A direct application of our proposed noisy measure  $\mathcal{M}(\theta, \mathcal{D}_{val})_{\hat{o}}$  in the WSOL setting is early stopping for model selection, and hyper-parameter search. In these applications, the measure must follow a similar behaviour to  $\mathcal{M}(\theta, \mathcal{D}_{val})_o$ , as shown in Fig.2.

**Pseudo-bbox annotation.** For generation of pseudo-bboxes (using  $\hat{o}$ ), we leverage pretrained-of-the-shelf region proposal models to generate LOC annotations for a held-out validation set  $\mathcal{D}_{val} = \{(x_i, y_i, \hat{o}(x_i))\}_{i=1}^N$ . This set is originally labeled with image-class labels only. These models can be unsupervised without the need for training or require weak supervision for training. We consider the three following scenarios of the pretrained model depending on its level of supervision.

(a) *Unsupervised*: In this case, the model does not have access to any supervision. Typical examples are conventional region proposal methods [9] that are generally

used to build pseudo-supervision to train object detector models [43]. SS [11] is a commonly used method where no parameters are learned. Carefully engineered features and score functions are used to greedily merge low-level superpixels that produce the final region proposals. The per-proposal score can be used to rank the likelihood that the proposal contains an object.

(b) *Supervised with image-class labels*: A middle-ground approach is to use image-class labels which are available in the WSOL setting. The CLIP model [10] is a model trained on millions of generic text-image pairs from the Internet. We use existing pretrained CLIP to pseudo-annotate our held-out  $\mathcal{D}_{val}$ . Class labels are used as a prompt to generate a CAM for the labeled object in the image. The CAM is automatically thresholded using the Otsu method [44]. Then, a bbox is constructed around each connected object. Since CLIP points to the discriminative region associated with the input image-class label, we select the largest bbox as a pseudo-bbox.

(c) *Supervised with class agnostic bboxes*: An alternative approach involves using a region proposal model that is trained using a general dataset like Pascal VOC and MSCOCO, with LOC bboxes. This methodology differs in that it does not employ image-class labels, but rather LOC bboxes that are class-agnostic. A typical example is the RPN [12], a fully convolutional network that simultaneously predicts object bounds at each position, and provides objectness scores that allow to rank proposals.

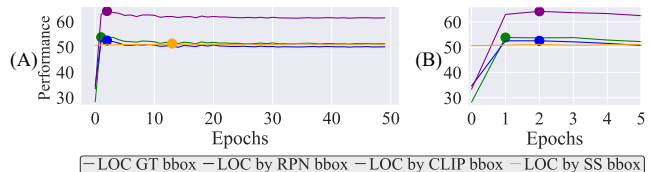


Figure 2: Model selection with early stopping at the epoch indicated with a dot using LOC accuracy. Different approaches are compared for pseudo-bbox annotation versus GT annotations (oracle). Fig(B) is a zoom of Fig.(A) between epochs 0 and 5. Results are reported over CUB validation set using the CAM method [42] with IoU as a LOC measure. LOC curves with pseudo-bbox annotations typically have similar behaviour to the oracle GT bbox annotations, making them suitable for WSOL model selection. They increase and reach their peak for a similar number of epochs, followed by a decline and stagnation in performance. In contrast, the CL curve reaches its peak toward the end of training when LOC performance has already degraded. CL accuracy is therefore inadequate as a WSOL selection criterion to achieve high LOC accuracy performance. Misalignment between LOC and CL behaviour has been studied further in [4].

For SS and RPN several bboxes are generated per image. To discard irrelevant bboxes and select the most discriminative one, we leverage the pointing game analysis [13] (see Fig.3). To this end, a classifier pretrained over  $\mathcal{D}_{train}$  is considered. It is trained until convergence using only image-class labels. The pointing game uses the maximum CAM response to select the most discriminative bboxes. In the case where multiple bboxes are ultimately selected, they are scored by the classifier response, and the bbox with the highest score is ultimately selected. Pseudo-bbox annotations are constructed for  $\mathcal{D}_{val}$ , where each box contains the most discriminative object labeled in the image. This process is only executed once before performing any WSOL training. The generated bboxes are stored on disk, and used for future WSOL training. Therefore, our approach does not add any computation time to the training itself.

Fig.2 shows the behaviour of LOC performance when using pseudo-bboxes vs oracle bboxes over  $\mathcal{D}_{val}$ . The overall trend is similar as they both increase during the first epochs and reach their peak, decline and stagnate over the following epochs. This is extremely helpful for early stopping and hyper-parameter search. We also observe that LOC using CLIP pseudo-annotation yields higher LOC than the with the oracle. This is plausible since a model prediction can be further aligned with some annotations than others.

To provide a realistic evaluation protocol for WSOL, we proposed a strategy to generate pseudo-bboxes for  $\mathcal{D}_{val}$ . It bypasses the need for manually annotated (oracle) bboxes by leveraging pretrained region proposal models. Then, the pointing game analysis is used to select the most discriminative proposals. In §4, we show that using manually annotated bboxes for  $\mathcal{D}_{val}$  set can increase LOC accuracy on  $\mathcal{D}_{test}$ , leading to performance overestimation. We also show that noisy pseudo-bboxes can effectively be used for model selection in the WSOL. This is initially shown using synthetic boxes, then using

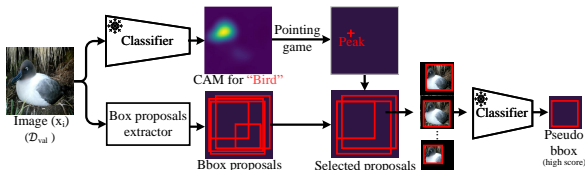


Figure 3: Our proposed LOC pseudo-bbox annotator  $\hat{\delta}$ . A set of bbox proposals is initially extracted using a region proposal model, and from them, discriminative ones are selected using pointing game analysis [13]. In the case where multiple bboxes are selected, the classifier confidence over the foreground region is used to select the most discriminative bbox.

our generated pseudo-bboxes. These pseudo-bboxes are made public to the researchers for the design of more realistic WSOL methods.

### 3.2 Threshold Estimation

WSOL methods seek to produce bboxes corresponding to particular objects. They generate a LOC map  $\mathcal{M} = \mathcal{M}^c \in \mathbb{R}^{H,W}$  highlighting the object of a class  $c$ , where  $\mathcal{M}_{ij}$  denotes the pixel value at location  $(i, j)$  for  $i \in \{1, 2, \dots, H\}$  and  $j \in \{1, 2, \dots, W\}$ . Higher values of  $\mathcal{M}_{ij}$  indicate the foreground and lower values indicate the background. The LOC map  $\mathcal{M}$  is first normalized due to varying score statistics across images. After normalization, WSOL methods apply a threshold  $\tau \in [0, 1]$  to  $\mathcal{M}$  to create a binary mask  $\{\mathcal{M}_{ij} \geq \tau\}$  for producing bbox. Conventionally, researchers either fix  $\tau$  or tune it as a hyperparameter. However, the optimal  $\tau$  varies based on the architecture and dataset. Choe et al. [4] proposed using multiple thresholds,  $\tau \in [0, 1]$ , to compute bboxes for different masks, and selecting the optimal threshold  $\tau^*$  based on performance statistics. While effective, this method tends to overestimate performance by using ground-truth bboxes for threshold estimation, which is unrealistic in the WSOL setting. Moreover, for  $\tau$  estimation, different automatic thresholding methods like OT<sup>4</sup> lead to an underestimation of performance, as they fail to consider the contextual relationships within the image. To address these issues, we propose using pseudo-bbox labels  $\hat{\delta}(x_i)$  produced by our method for  $\tau$  estimation. This approach is more realistic and achieves performance that is competitive to the case where  $\tau$  is estimated with the test set.

## 4 Experimental Validation

### 4.1 Methodology

**Datasets.** In our experiments, two challenging datasets are employed, widely recognized for the validation of WSOL models. They are, (i) **CUB** [45], encompasses 200 classes with a total of 11,788 images. These are divided into 5,994 images for training and 5,794 for testing. Additionally, for validation, we employed an independent validation set comprising 1,000 images representing five per class, as provided by [4]. (ii) **ILSVRC** [46] consists of approximately 1.2 million images for training and 10,000 images for the validation set, distributed across 1,000 classes. We utilized the validation split in-

<sup>4</sup>OT evaluates all possible threshold values, calculates the variance within each of the two clusters (background and foreground), and selects the threshold that minimizes the weighted sum of these variances.

cluded with the original dataset as our test set, given its ample sample size suitable for testing. However, for validation, we utilized **ILSVRC-V2**, collected by [47] and annotated by [4], which minimizes biases toward the test set. Moreover, to ensure a consistent and fair comparison, we closely adhered to the dataset-splitting strategy proposed by [4] for both datasets.

**WSOL methods.** To compare the performance of the proposed protocol, we employed eight state-of-the-art WSOL methods, which include CAM [42], HaS [7], ACoL [8], ADL [6], NL-CCAM [48], TS-CAM [2] SCM [1], and SAT [3]. Further details regarding these methods can be found in the supplementary material.

**Implementation details.** For each dataset, we adopted a uniform batch size of 32, and resized each image to a size of  $256 \times 256$  pixels and then employed random cropping to  $224 \times 224$  pixels followed by random horizontal flipping. Experiments were performed on 50 training epochs for CUB and 10 for ILSVRC. Furthermore, each method was trained using the stochastic gradient descent optimizer while utilizing four shared hyperparameters for each method: learning rate, step size, weight decay, and gamma. For these shared hyperparameters, a total of 180 configurations were chosen. Additionally, for different methods, specific parameters were selected from their feasible range, and a cartesian product of these hyperparameters with the shared ones was computed to produce the final grid for hyperparameter<sup>5</sup> optimization. This extensive set of configurations, substantially larger than the scope explored in prior studies, e.g. Choe et al. (2020), provides more fair comparisons among the different methods. Moreover, to study the impact of noisy bboxes on the model selection, we train CAM on CUB until 100 epochs, exploring 1,080 configurations using common hyperparameters.

## 4.2 Results and Discussions

**(1) Model selection with noisy ground truth bboxes.** This section presents an initial results designed to validate the robustness of the proposed model selection techniques. We systematically perturbed the GT bbox, initially employed for model selection, to simulate the scenario for noisy or imprecise GT annotations. The primary aim is to evaluate the sensitivity of model selection to errors in the GT bbox. *The objective is to determine whether growing degrees of GT bboxes noise affects model selection performance?* Positive results would substantiate the reliability of our model selection mechanism under real-world inaccuracies in bbox anno-

<sup>5</sup>The comprehensive details on the hyperparameter space are included in the supplementary material.

Annotator	CUB	ILSVRC
SS + Proposed bbox selection	39.98	45.07
RPN + Proposed bbox selection	71.23	61.08
CLIP + Proposed bbox selection	68.80	64.41

Table 1: IoU performance of generated pseudo-bboxes w.r.t GT bboxes on the validation set.

tations. Our experiments encompass ten noise levels (see Fig.4A), and involve 300 experiments using the CAM method with perturbed bboxes for validation set model selection. Our findings reveal that the WSOL method maintains its localization performance even with very noisy validation set bboxes (Fig.4B). This suggests that model selection can be effectively performed with coarse localization cues. The selection frequency across different epochs using GT and noisy bboxes is remarkably similar (Fig.4D). In Fig.4C histogram comparing model selection epochs using GT and noisy bboxes indicates a central tendency around zero, showing that coarse GT bboxes from various sources enable reliable model selection while sustaining a high level of accuracy. *More information regarding the generation of bboxes can be found in supplement materials.*

### (2) Generation of pseudo-GT bboxes.

Three different off-the-shelf models, SS, RPN, and CLIP, are employed for generating pseudo-bboxes. Since, these methods generate a set class-agnostic pseudo-bboxes and *pointing game* is employed for selecting discriminative boxes. This involves harvesting CAM from a pretrained classifier, pinpointing the peak activation, and evaluating its spatial overlap with annotated GT-bboxes. A successful LOC of pointing game is counted if the peak activation in CAMs overlaps with annotated bboxes, using  $\frac{Hits}{Hits+Misses}$ . The pointing game accuracy of pretrained classifier’s CAMs used to filter discriminative bboxes, achieving 98.70% accuracy on the CUB validation split, 98.00% on the test split, 88.05% on the ILSVRC validation split, and 89.03% on the test split.

Details about generating pseudo-bboxes  $\hat{\delta}(x_i)$  is presented in §3, and the IoU accuracy of the pseudo-bboxes w.r.t. GT bboxes on the validation set is reported in Tab.1. Despite the noise, these pseudo-boxes are expected to be useful for model selection and threshold estimation, as demonstrated in the previous section. Examples of pseudo-bboxes generated by RPN and SS are shown in Fig.4E.

**(3) Pseudo-bboxes and  $\tau$  estimation.** We employed our proposed model selection protocol across different region proposal methods as outlined in §4.1. During the training of each method, we employed a validation set for model selection with which encompassed image, class labels, pseudo-bboxes generated by different off-the-shelf

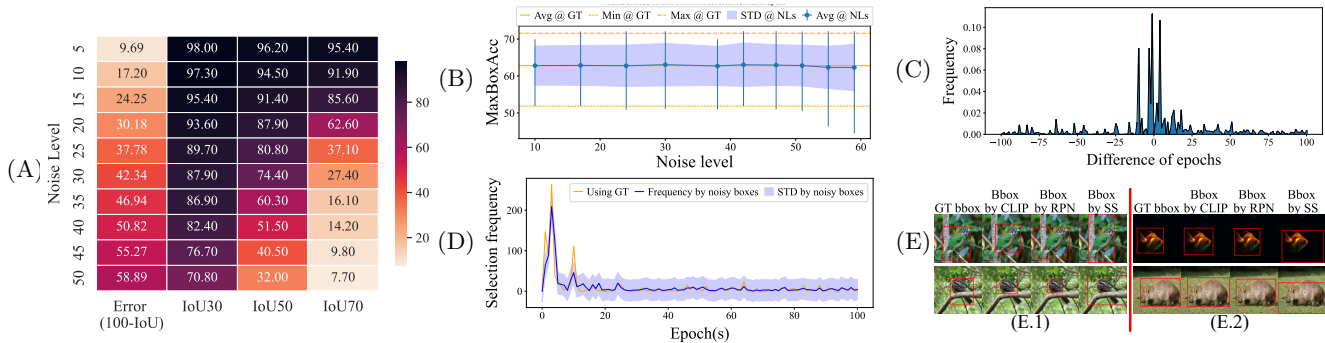


Figure 4: (A) The heatmap illustrates the inaccuracies in noisy bboxes at various noise levels generated by augmenting GT bboxes. (B) The blue line represents the average LOC accuracy over various configurations on the test set, incorporating maxima, minima, and standard deviation; the model is selected using a validation set comprising noisy bboxes with varying noise levels. In contrast, orange lines represent the average maximum and minimum performance of a model chosen during hyperparameter optimization over GT for configurations analogous to those employed with noisy labels. (C) Histogram illustrating the variance in model selection epochs when using bboxes at various noise levels w.r.t ground truth boxes for experiments with identical configurations, highlighting a tendency around zero. (D) Model selection epoch frequency using GT and noisy boxes across different configurations and noise levels. (E) Illustration of pseudo-bboxes along with the GT over (E.1) CUB and (E.2) ILSVRC validation set.

methods. We compared the performance of the models trained with these pseudo-bboxes against those trained with ground truth bboxes. For every region proposal method, we selected a model using validation accuracy. Its performance was tested using a test set, and then the best-performing model was selected using the same type of supervision used to select the best on the validation set. The results from these experiments are reported in Tab.2, where WSOL models employing pseudo label bboxes for model selection achieved results comparable to those using GT bboxes. This suggests that reliable model selection is possible with coarse bboxes.

Results also show that selecting models based on best validation (BV) across different hyperparameter configurations yields competitive results and is a more realistic approach when compared to the model selected using best test (BT) accuracy. Furthermore, when the best model is selected using pseudo-bboxes  $\hat{o}(x_i)$  and the threshold  $\tau$  is estimated using  $\hat{o}(x_i)$  (BV-VT), we achieve accuracy comparable to methods that utilize manual bbox annotations for validation, and use the BT for  $\tau$  estimation (BT-TT). *This indicates that model selection should be based on validation set performance across different experiments, avoiding overestimating model performance.*

Additionally, if the foreground saliency mask predictor [49] is employed to fit oracle bboxes (converted into a binary map) over the  $\mathcal{D}_{val}$ , it achieves a MaxBoxAcc of 68.7% and 94.0% on the ILSVRC and CUB, respectively [4]. Performance is comparable to models trained in

the WSOL setting, which utilize a much larger  $\mathcal{D}_{train}$  and  $\mathcal{D}_{val}$  for model selection. Our results also suggest that the pseudo-box annotation  $\mathcal{D}_{val}$  should be used for model evaluation and  $\tau$  estimation.

(4) **Recommendation for realistic evaluation.** In line with our proposed evaluation protocol and empirical results, we recommend the following practices. Training and evaluation should be constrained to only utilizing class-level labels without resorting to manual bbox annotations for model selection and threshold estimation: (i) We recommend utilizing pseudo-bboxes generated by off-the-shelf methods for validation set. Our experiments show that these pseudo-bboxes can effectively provide the LOC annotation for model selection, achieving performance comparable to using GT annotations. (ii) Estimating thresholds using pseudo-bboxes from the validation set instead of the test set to produce bboxes from LOC maps. This approach addresses the unrealistic practice of thresholding. (iii) Our experiments suggest that model selection across various experiments, each employing different hyperparameters, should be based on the performance of pseudo-bboxes on the validation set. This approach mitigates bias in model performance evaluation. (iv) Be cautious when using thresholded-IoU metrics (IoU-30, IoU-50, IoU-70) and their variants, as these can mislead by considering uniform performance across instances above the set threshold. Our analysis reveals a non-linear relationship between thresholded-IoU and IoU (Tab.3). We recommend the use of non-thresholded-IoU for realistic evaluation.



		CUB (MaxBoxAcc)					ILSVRC (MaxBoxAcc)				
Method	Select	CL	GT	RPN	CLIP	SS	CL	GT	RPN	CLIP	SS
CAM [42] ( <i>cupr'16</i> ) ResNet50	BT-TT	32.99	70.40	71.10	70.62	69.89	46.29	64.06	63.60	63.90	63.60
	BT-VT	—	69.50	70.43	69.88	27.97	—	63.90	62.89	63.88	46.97
	BV-TT	29.37	70.40	70.40	69.76	61.20	46.83	64.06	63.60	64.01	63.60
	BV-VT	—	69.20	68.93	67.98	22.79	—	63.88	62.89	63.88	45.91
HaS [7] ( <i>iccv'17</i> ) ResNet50	BT-TT	37.00	75.85	75.85	75.85	74.73	37.82	63.77	63.94	63.77	63.30
	BT-VT	—	74.68	75.69	75.69	25.42	—	63.86	62.08	63.28	49.02
	BV-TT	30.11	75.49	74.92	73.38	72.69	45.80	63.94	63.34	63.54	63.30
	BV-VT	—	74.68	74.02	73.24	22.43	—	63.86	62.08	63.06	48.21
ACoL [8] ( <i>cupr'18</i> ) ResNet50	BT-TT	46.59	74.64	74.64	75.37	74.14	50.46	62.93	62.75	63.45	62.92
	BT-VT	—	73.50	73.83	74.83	33.43	—	63.48	61.61	63.47	52.38
	BV-TT	34.89	74.64	74.64	72.29	56.04	50.46	63.70	62.75	62.93	62.92
	BV-VT	—	73.50	73.83	72.21	27.85	—	63.48	61.31	62.80	52.38
ADL [6] ( <i>cupr'19</i> ) ResNet50	BT-TT	40.97	76.63	76.63	76.06	74.99	39.80	65.11	65.97	65.11	65.19
	BT-VT	—	76.21	76.52	75.92	27.39	—	65.2	64.29	65.04	49.61
	BV-TT	37.17	75.83	75.97	75.80	32.08	44.23	65.28	65.18	65.32	65.06
	BV-VT	—	72.73	75.85	74.73	22.21	—	65.2	62.30	65.04	47.09
CCAM [48] ( <i>wacv'20</i> ) VGG	BT-TT	52.67	65.58	65.58	65.22	45.97	49.80	60.63	60.63	60.63	52.72
	BT-VT	—	64.44	65.27	62.54	31.89	—	60.52	60.52	60.56	46.63
	BV-TT	52.67	65.58	65.58	65.22	45.97	49.80	60.63	60.63	60.63	52.72
	BV-VT	—	62.44	64.84	62.54	31.89	—	60.52	60.52	60.56	46.63
TS-CAM [2] ( <i>iccv'21</i> ) DeiT-S	BT-TT	51.77	90.19	90.35	89.52	88.71	6.476	66.75	66.75	66.75	66.17
	BT-VT	—	89.33	90.16	89.52	29.49	—	66.65	65.12	65.32	47.63
	BV-TT	39.17	89.52	89.52	89.16	77.39	6.476	66.75	66.14	66.75	55.7
	BV-VT	—	88.85	88.90	88.95	24.19	—	66.65	64.97	65.32	46.80
SCM [1] ( <i>eccv'22</i> ) DeiT-S	BT-TT	30.82	91.56	92.25	92.26	91.76	47.55	61.76	61.75	61.75	59.76
	BT-VT	—	90.26	92.00	92.16	26.44	—	61.76	61.15	61.38	49.27
	BV-TT	30.82	91.56	92.25	92.26	80.16	47.55	61.76	61.75	61.75	59.76
	BV-VT	—	90.26	92.00	92.16	22.02	—	61.76	60.21	61.38	49.27
SAT [3] ( <i>iccv'23</i> ) DeiT-S	BT-TT	69.60	92.14	92.45	91.45	92.23	64.59	70.12	67.08	70.13	70.13
	BT-VT	—	91.66	92.26	91.00	41.62	—	69.46	64.78	69.05	57.06
	BV-TT	70.24	91.33	91.75	89.97	91.33	66.17	70.12	67.08	70.13	70.13
	BV-VT	—	90.86	91.71	89.93	28.04	—	69.46	64.78	69.05	57.06

Table 2: Test-set MaxBoxAcc of WSOL models with different selection criteria on CUB and ILSVRC. The *select* column presents (i) BT and BV indicate model selection based on hyperparameter configurations using the test set and validation set, respectively; (ii) TT and VT indicate that the threshold  $\tau$  is selected using either the test set or validation set. For model selection on the validation set, we consider the GT as a reference, a selection based on the CL performance and the three different pseudo-bboxes generation proposed in this work: RPN, CLIP and SS. Our results for models selected with pseudo-bboxes are comparable to those of GT.

Method	CUB-200-2011		ILSVRC	
	MaxBoxAcc (IoU-50)	IoU	MaxBoxAcc (IoU-50)	IoU
CAM [42]	70.40	56.71	64.06	57.89
HaS [7]	75.85	59.81	63.77	58.49
ACoL [8]	74.64	58.29	62.93	56.39
ADL [6]	76.63	60.12	65.11	58.46
NL-CCAM [48]	65.58	54.76	60.63	54.98
TS-CAM [2]	90.19	69.78	66.75	59.54
SCM [1]	91.56	70.27	61.76	54.55
SAT [3]	92.14	73.67	70.12	62.80

Table 3: Analysis of MaxBoxAcc (IoU-50) versus IoU using oracle bboxes for model selection. Analysis using pseudo-bboxes is presented in *supplementary material* exhibiting same behaviour.

## 5 Conclusion

The current protocol [4] has brought significant progress in the evaluation of WSOL methods. However, its reliance on manually annotated bboxes during validation for model selection, and annotated test set for threshold estimation leads to an overestimation of localization performance over the test set. In this work, we propose the generation of pseudo-bboxes for the validation set using off-the-shelf pretrained region proposal models for both model selection and threshold estimation. This threshold is then employed to produce bboxes from L0C maps on the test set. Our approach, evaluated across different WSOL methods, demonstrates that employing pseudo-bboxes for model evaluation achieves localization performance comparable to models selected using oracle bboxes and threshold is estimated on test set. This is, therefore, a promising and more realistic alternative than using a GT annotated held-out dataset. Despite the promising results with our protocol, performing model selection in WSOL without L0C annotation remains an open issue.

## A Supplementary material

This includes descriptions of evaluated methods, steps to generate noisy GT bboxes, the performance of pseudo-bboxes at different selection steps, and an analysis of measures (thresholded-IoU vs. IoU).

This supplementary material contains the following content:

### A.1. Review of evaluated methods and their search spaces.

**A.1.1. Evaluated methods.** In this section, we provided a detailed description of methods employed to evaluate the efficacy of our proposed protocol for model selection.

**A.1.2. Hyperparameter search space.** This part describes various hyperparameters for each method, along with their respective feasible range.

### A.2. Generation of noisy ground truth bboxes.

This section delineates the methodology for generating noisy ground truth (GT) bounding boxes (bboxes) to analyze their impact on model selection.

### A.3. Pseudo-bboxes performance across different selection steps.

This section presents the performance of pseudo-bboxes at different selection steps of our proposed method.

**A.4. Localization evaluation in WSOL (thresholded-IoU vs IoU).**: This section describes an ongoing challenge in WSOL where discrepancies in localization performance exist between the commonly used `MaxBoxAcc` and the IoU metric.

## A.1 Review of Evaluated Methods and their Search Spaces

### A.1.1 Evaluated Methods

To assess the efficacy of the proposed protocol, we employ eight methods published in top-tier venues from 2016 to 2023. These methods are presented chronologically within this section, providing a comprehensive overview.

**Class activation mapping (CAM)** [42] is able to extract an activation map for a particular class using a pre-trained CNN-classifier with global average pooling. It generates the final map by aggregating different activation maps from the penultimate convolution layer based on the contribution towards each class by using weights from the last fully connected layer.

**Hide-and-see (HaS)** [7] force the network to look beyond discriminative regions of a particular object by augmenting the input image. It hides patches of input image during training by employing two hyperparameters; drop rate and grid size.

**Adversarial complementary learning (ACoL)** [8] employees an architecture with two parallel classifier heads that tires to find complementary regions by adversarially erasing high-scoring activations.

**Attention-based dropout layer (ADL)** [6] works similarly as ACoL by erasing high-score activation to force by employing drop masks generated without second classifiers head.

**Non-local combinational class activation maps (NL-CCAM)** [48]. In this paper, the author argues that employing the activation map of the class with the highest classifier’s score may only highlight discriminative regions and for certain images it tends to focus on background regions. To address this limitation, the author proposes to combine activation maps of different classes. This combination is based on the respective probability score of each, encompassing a spectrum from the highest to the lowest.

**Token semantic coupled attention map (TS-CAM)** [2]. TS-CAM is a cascaded ViT-CNN architecture that proposes to redistribute class information to patch tokens. This is achieved by implementing a

CNN-based classification (CL) head atop the patch tokens, thereby rendering the CLS token class-agnostic. Therefore, these CLS tokens are combined with the activation map extracted from the last convolutional layer to produce an activation map highlighting different object parts of a particular class.

**Spatial calibration module (SCM)** [1]. This paper introduced an SCM module atop the transformer features to align the boundaries of the generated map with the object boundaries by avoiding partial activation in different areas of the activation map. This module integrates semantic similarities presented in patch tokens and their spatial relationships into a unified model. SCM effectively recalibrates the transformer’s attention and semantic representations to mitigate the background noise and sharpen object boundaries.

**Task-specific spatial-aware token (SAT).** [3] This paper introduces a spatial-aware token (SAT) into the transformer’s input space. Like CLS token that is able to accumulate information for CL tasks, it is incorporated to aggregate the global representation of the object of interest. Furthermore, the SAT is a passed-to spatial-query attention module that treats the SAT as a query to calculate similarity with different patches and produces probabilities for foreground object for producing accurate localization maps.

### A.1.2 Hyperparamter Search Space

To fairly compare different WSOL methods, we took steps to minimize human biases during training. This includes employing pseudo-bboxes for the evaluation and sampling hyperparameter values from the feasible range, except for annotations on the test set, which were used only to assess the trained model’s performance.

Each method was trained using four shared hyperparameters, while the additional hyperparameters were specific to each model. We sampled the values for these hyperparameters from their feasible range. A cartesian product of these and shared hyperparameters was computed to create the final grid of hyperparameters for training each model. A detailed summary of the hyperparameters employed to train different WSOL models is presented in Tab.A1.

## A.2 Generation of Noisy Ground Truth Bboxes

In the main paper, we introduce a validation protocol designed to evaluate the robustness of the proposed model selection techniques in the presence of noisy GT bboxes. This protocol systematically perturbs the GT bboxes,

Method	Hyperparameter	Sampling Distribution	Range
Common HPs	LR, WD, Gamma	LogUniform	$[10^{-5}, 10^0]$
	Step Size	Uniform	CUB: $[5 - 45]$ ILSVRC: $[2 - 9]$
CAM [42], TS-CAM [2] SCM [1], NL-CCAM [48]	Common HPs	-	-
HaS [7]	Drop Rate, Drop Area	Uniform	$[0, 1]$
ACoL [8]	Erasing Threshold	Uniform	$[0, 1]$
ADL [6]	Drop Rate, Erasing Threshold	Uniform	$[0, 1]$
SAT [3]	Area Threshold	Uniform	$[0, 1]$

Table A1: Hyperparameter search space for different methods

initially used for model selection, to emulate conditions of noisy or imprecise GT annotations. To produce noisy GT bboxes, a sequence of random transformations is applied to the GT bboxes, creating varying noise levels. For each transformation, a total of ten unique noise levels are defined. These levels signify the maximum likelihood of deformation at each noise level. This likelihood is derived by sampling the deformation value using a uniform distribution that varies from 5 to 50, with intervals set at 5. To generate noisy bboxes we, first apply, scaling transformation to the GT bboxes between -50% and +50% with a maximum likelihood of a particular noise level. Following the scaling, we apply shift transformation to the scaled bbox by choosing a random shift length, where the shift length is set between 0% and the maximum size percentage corresponding to a particular noise level. Finally, we modify the aspect ratio of bbox based on a probability factor ‘p’ which indicates the likelihood, representing a specific noise level.

### A.3 Pseudo-bboxes Performance Across Different Selection Steps

Different off-the-shelf models, SS, RPN, and CLIP, are employed to produce pseudo-bboxes. These methods generate a set of class-agnostic pseudo-bboxes. To select discriminative boxes from a pool of object proposals, the pointing game analysis was employed [13]. This involves harvesting CAM from a pre-trained classifier and pinpointing the peak activation that is used to select discriminative boxes. Despite the initial filtering of bboxes via the pointing game, a substantial number of bboxes remained. To address this, we employ a sequential refinement process, in which we initially filter the top 20% based on objectness or classifier score for boxes obtained from RPN and SS, respectively. Subsequently, the pointing game was employed to refine this selection, followed by selection of top-performing boxes based on score. In the case of CLIP, we utilized Otsu’s thresholding method to identify binary maps, upon which bboxes were delineated around the largest connected areas. A

Method	CUB (IoU)			ILSVRC (IoU)		
	SS	RPN	CLIP	SS	RPN	CLIP
Mean IoU (PG*)	32.21	28.71	-	23.38	27.57	-
Mean IoU (PG*, 20% Filtered)	33.69	37.89	-	34.99	37.17	-
Mean IoU (Top Box, 20% by Objectness Score)	39.90	69.80	-	44.90	54.02	-
Mean IoU (Top Box, 20%, PG*+Scoring)	39.98	71.23	-	45.07	61.08	-
Upper Bound (Select by IoU with GT)	64.07	83.66	-	65.46	84.42	-
IoU from Otsu	-	-	68.80	-	-	64.41
IoU using 1K Threshold	-	-	69.56	-	-	65.78

\*PG: Pointing Game

Table A2: Performance of pseudo-bboxes obtained using different off-the-shelf region proposal methods across multiple refinement stages over the validation set. The table highlights the incremental improvement in IoU through various selection steps.

comprehensive description of the proposed method for generating pseudo-bboxes is provided in the main paper.

The performance of pseudo-bboxes at different selection steps is presented in Tab.A2. This table shows that as we select relevant bboxes generated by SS or RPN at each stage, we progressively choose better-performing bboxes, resulting in reliable performance relative to the upper bound performance when using GT bboxes to select top-performing bbox. Initially, pseudo-bboxes generated by SS and RPN are filtered based on objectness or classifier scores, followed by a pointing game analysis for further refinement. The results indicate a significant improvement in the mean intersection over union (IoU) across these selection stages. For example, after the initial selection and filtering of the top 20% based on objectness scores, the IoU increases substantially, demonstrating the efficacy of our proposed method. In contrast, CLIP generates activation maps that highlight particular objects. Otsu’s thresholding method is employed to convert these maps into binary images, enabling the delineation of bboxes around the largest connected areas. Despite the single-stage selection process for CLIP-generated maps, the resulting bounding boxes achieve competitive performance.

### A.4 Localization Evaluation in WSOL (Thresholded-IoU vs IoU)

So far, we have reported the localization performance using MaxBoxAcc metric [4]. It is also known as as *GT-known localization* metric. It scores one point when the IoU between the GT bbox and the predicted box is above 50%, otherwise, it scores 0. It is referred to IoU 5-0 as well. It is a well established and commonly used metric in WSOL. In addition to IoU-50, we report the IoU in Tab.3 of the main paper. These results show that model

Method	Backbone	CUB-200-2011 (MaxBoxAcc)					CUB-200-2011 (IoU)					ILSVRC (MaxBoxAcc)					ILSVRC (IoU)				
		CL	GT	RPN	CLIP	SS	CL	GT	RPN	CLIP	SS	CL	GT	RPN	CLIP	SS	CL	GT	RPN	CLIP	SS
CAM [42] (cvpr,2016)	ResNet50	66.98	70.40	71.10	70.62	69.89	55.53	56.71	56.88	56.65	56.76	61.48	64.06	63.60	63.90	63.60	56.17	57.89	57.42	57.68	57.42
HaS [7] (iccv,2017)	ResNet50	67.62	75.85	75.85	75.85	74.73	57.01	59.81	59.81	59.81	59.39	61.69	63.77	63.94	63.77	63.30	56.81	58.49	58.39	58.49	57.32
ACoL [8] (cvpr,2018)	ResNet50	66.62	74.64	74.64	75.37	74.14	55.32	58.29	58.29	58.55	58.13	61.98	62.93	62.75	63.45	62.92	55.62	56.39	56.32	56.94	56.39
ADL [6] (cvpr,2019)	ResNet50	67.82	76.63	76.63	76.06	74.99	55.64	59.12	59.12	58.93	58.32	62.81	65.11	65.97	65.11	65.19	56.39	58.46	58.37	58.55	58.54
NL-CCAM [48] (wacv,2020)	VGG-GAP	64.15	65.58	65.58	65.22	45.97	54.11	54.76	54.76	54.59	47.88	58.42	60.63	60.63	60.63	52.72	51.59	54.98	54.98	54.98	49.44
TS-CAM [2] (iccv,2021)	DeiT-S	88.36	90.19	90.35	89.52	88.71	69.14	69.78	69.83	69.95	68.36	56.40	66.75	66.75	66.75	66.17	53.67	59.54	59.54	59.54	59.00
SCM [1] (eccv,2022)	DeiT-S	88.47	91.56	92.25	92.26	91.76	68.64	70.27	70.89	70.93	70.34	57.92	61.76	61.75	61.75	59.76	52.13	54.55	54.56	54.56	53.47
SAT [3] (iccv,2023)	DeiT-S	79.70	92.14	92.45	91.45	92.23	63.13	73.67	73.59	72.92	73.61	64.94	70.12	67.08	70.13	70.13	56.09	62.80	58.55	62.80	62.80

Table A3: Comparative Analysis of MaxBoxAcc (IoU-50) versus IoU on CUB and ILSVRC with different model selection methods.

selection using CL accuracy still lead to poor IoU. However, selection using our proposed pseudo-bboxes yields competitive IoU compared to when using oracle bboxes.

The comparison based on IoU (Tab.3 of the main paper) lead us to an interesting result presented in Tab.A3. This table shows that MaxBoxAcc, using the commonly oracle bboxes, gives largely higher localization scores compared to the exact localization accuracy reported by IoU. For instance, SAT method [3] scores 92.14% in MaxBoxAcc, while it only scores 73.12% over CUB dataset. When considering only MaxBoxAcc, the results give the impression that CUB dataset is saturated, especially when the same authors [3] have reported a MaxBoxAcc of 98.45%. However, when inspecting IoU metric, localization is still low at 73.12%.

In addition, since MaxBoxAcc is based on thresholding, extreme localization scores can hit the same scoring point. For instance, a prediction with IoU = 50.1% scores the same point as when the prediction is IoU = 99.99%. However, both IoU = 49.9%, IoU = 1% scores 0 point in MaxBoxAcc. This makes localization evaluation less efficient.

Despite its common usage in the literature, the aforementioned limitations of MaxBoxAcc suggest that reporting IoU along with MaxBoxAcc could be beneficial in better assessing localization performance of different methods in WSOL.

Since CUB dataset is relatively easier than ILSVRC dataset, the latter paints a realistic evaluation of the progress that has been done in WSOL. Since the work of Zhou et al. [42] in 2016 up to now, only  $\approx 6\%$ , and  $\approx 4.9\%$  of improvement has been done in term of MaxBoxAcc and IoU, respectively. This suggests that a lot of work is till needs to be done to furthermore improve WSOL methods.

## References

[1] H. Bai, R. Zhang, J. Wang, and X. Wan, “Weakly supervised object localization via transformer with implicit

spatial calibration,” *ECCV*, 2022. 1, 7, 9, 10, 11, 12

- [2] W. Gao, F. Wan, X. Pan, Z. Peng, Q. Tian, Z. Han, B. Zhou, and Q. Ye, “Ts-cam: Token semantic coupled attention map for weakly supervised object localization,” in *ICCV*, 2021. 7, 9, 10, 11, 12
- [3] P. Wu, W. Zhai, Y. Cao, J. Luo, and Z. Zha, “Spatial-aware token for weakly supervised object localization,” in *ICCV*, 2023. 1, 2, 7, 9, 10, 11, 12
- [4] J. Choe, S. Oh, S. Lee, S. Chun, Z. Akata, and H. Shim, “Evaluating weakly supervised object localization methods right,” in *CVPR*, 2020. 1, 2, 4, 5, 6, 7, 8, 9, 11
- [5] J. Rony, S. Belharbi, J. Dolz, I. Ben Ayed, L. McCaffrey, and E. Granger, “Deep weakly-supervised learning methods for classification and localization in histology images: A survey,” *Machine Learning for Biomedical Imaging*, vol. 2, pp. 96–150, 2023. 1
- [6] J. Choe and H. Shim, “Attention-based dropout layer for weakly supervised object localization,” in *CVPR*, 2019. 2, 4, 7, 9, 10, 11, 12
- [7] K. K. Singh and Y. J. Lee, “Hide-and-seek: Forcing a network to be meticulous for weakly-supervised object and action localization,” in *ICCV*, 2017. 7, 9, 10, 11, 12
- [8] X. Zhang, Y. Wei, J. Feng, Y. Yang, and T. Huang, “Adversarial complementary learning for weakly supervised object localization,” in *CVPR*, 2018. 2, 4, 7, 9, 10, 11, 12
- [9] J. Hosang, R. Benenson, and B. Schiele, “How good are detection proposals, really?,” in *BMVC*, 2014. 2, 5
- [10] Y. Lin, M. Chen, W. Wang, B. Wu, K. Li, B. Lin, H. Liu, and X. He, “CLIP is also an efficient segmenter: A text-driven approach for weakly supervised semantic segmentation,” in *CVPR*, 2023. 2, 3, 5
- [11] J. Uijlings, K. Van De Sande, T. Gevers, and A. Smeulders, “Selective search for object recognition,” *IJCV*, vol. 104, pp. 154–171, 2013. 2, 3, 5
- [12] S. Ren, K. He, R. Girshick, and J. Sun, “Faster r-cnn: Towards real-time object detection with region proposal networks,” *NeurIPS*, 2015. 2, 3, 5

- [13] J. Zhang, S. A. Bargal, Z. Lin, J. Brandt, X. Shen, and S. Sclaroff, "Top-down neural attention by excitation backprop," *IJCV*, vol. 126, no. 10, pp. 1084–1102, 2018. [2](#), [6](#), [11](#)
- [14] W. Finnoff, F. Hergert, and H. Zimmermann, "Improving model selection by nonconvergent methods," *Neural Networks*, vol. 6, no. 6, pp. 771–783, 1993. [3](#)
- [15] A. Lodwich, Y. Rangoni, and T. M. Breuel, "Evaluation of robustness and performance of early stopping rules with multi layer perceptrons," in *IJCNN*, 2009.
- [16] N. Morgan and H. Boullard, "Generalization and parameter estimation in feedforward nets: Some experiments," *NeurIPS*, vol. 2, 1989. [3](#)
- [17] V. Cheplygina, M. de Bruijne, and J. Pluim, "Not-so-supervised: a survey of semi-supervised, multi-instance, and transfer learning in medical image analysis," *Medical image analysis*, vol. 54, pp. 280–296, 2019. [3](#)
- [18] Z.-H. Zhou, "A brief introduction to weakly supervised learning," *National science review*, vol. 5, no. 1, pp. 44–53, 2018. [3](#)
- [19] A. Oliver, A. Odena, C. Raffel, E. D. Cubuk, and I. Goodfellow, "Realistic evaluation of deep semi-supervised learning algorithms," in *NeurIPS*, 2018. [3](#)
- [20] J. Su, Z. Cheng, and S. Maji, "A realistic evaluation of semi-supervised learning for fine-grained classification," in *CVPR*, 2021. [3](#)
- [21] M. Dinu, M. Holzleitner, M. Beck, H. D. Nguyen, A. Huber, H. Eghbal-zadeh, B. A. Moser, S. V. Pereverzyev, S. Hochreiter, and W. Zellinger, "Addressing parameter choice issues in unsupervised domain adaptation by aggregation," in *ICLR*, 2023. [3](#)
- [22] L. Ericsson, D. Li, and T. M. Hospedales, "Better practices for domain adaptation," in *AutoML*, 2023. [3](#)
- [23] K. Saito, D. Kim, P. Teterwak, S. Sclaroff, T. Darrell, and K. Saenko, "Tune it the right way: Unsupervised validation of domain adaptation via soft neighborhood density," in *ICCV*, 2021.
- [24] T. Salvador, K. FATRAS, I. Mitliagkas, and A. M. Oberman, "A reproducible and realistic evaluation of partial domain adaptation methods," in *NeurIPS Workshop on Distribution Shifts: Connecting Methods and Applications*, 2022.
- [25] J. Yang, H. Qian, Y. Xu, and L. Xie, "Can we evaluate domain adaptation models without target-domain labels?," *CoRR*, vol. abs/2305.18712, 2023. [3](#)
- [26] K. You, X. Wang, M. Long, and M. I. Jordan, "Towards accurate model selection in deep unsupervised domain adaptation," in *ICML* (K. Chaudhuri and R. Salakhutdinov, eds.), 2019. [3](#)
- [27] Y. Shi and F. Sha, "Information-theoretical learning of discriminative clusters for unsupervised domain adaptation," in *ICLM*, 2012. [3](#)
- [28] Y. Fang, P. Yap, W. Lin, H. Zhu, and M. Liu, "Source-free unsupervised domain adaptation: A survey," *CoRR*, vol. abs/2301.00265, 2023. [3](#)
- [29] M. Caron, H. Touvron, I. Misra, H. Jégou, J. Mairal, P. Bojanowski, and A. Joulin, "Emerging properties in self-supervised vision transformers," in *ICCV*, pp. 9650–9660, 2021. [3](#)
- [30] W. Chen and M. L. Cummings, "Subjectivity in unsupervised machine learning model selection," *CoRR*, vol. abs/2309.00201, 2023. [3](#)
- [31] S. Vaithyanathan and B. Dom, "Generalized model selection for unsupervised learning in high dimensions," in *NeurIPS*, 1999. [3](#)
- [32] A. Borji, "Pros and cons of GAN evaluation measures," *Computer Vision and Image Understanding*, vol. 179, pp. 41–65, 2019. [3](#)
- [33] M. Heusel, H. Ramsauer, T. Unterthiner, B. Nessler, and S. Hochreiter, "Gans trained by a two time-scale update rule converge to a local nash equilibrium," in *NeurIPS*, 2017. [3](#)
- [34] T. Salimans, I. Goodfellow, W. Zaremba, V. Cheung, A. Radford, and X. Chen, "Improved techniques for training gans," in *NeurIPS*, 2016.
- [35] R. Zhang, P. Isola, A. A. Efros, E. Shechtman, and O. Wang, "The unreasonable effectiveness of deep features as a perceptual metric," in *CVPR*, 2018. [3](#)
- [36] M. Mahseerici, L. Balles, C. Lassner, and P. Hennig, "Early stopping without a validation set," *CoRR*, vol. abs/1703.09580, 2017. [4](#)
- [37] D. Duvenaud, D. Maclaurin, and R. Adams, "Early stopping as nonparametric variational inference," in *Artificial intelligence and statistics*, pp. 1070–1077, 2016. [4](#)
- [38] S. Yuan, L. Feng, and T. Liu, "Early stopping against label noise without validation data," in *ICLR*, 2024. [4](#)
- [39] W. Li, C. Geng, and S. Chen, "Leave zero out: Towards a no-cross-validation approach for model selection," *CoRR*, vol. abs/2012.13309, 2020. [4](#)
- [40] D. Bonet, A. Ortega, J. R. Hidalgo, and S. Shekkizhar, "Channel-wise early stopping without a validation set via NNK polytope interpolation," in *APSIPA*, 2021. [4](#)
- [41] S. Shekkizhar and A. Ortega, "Deepnnk: Explaining deep models and their generalization using polytope interpolation," *CoRR*, vol. abs/2007.10505, 2020. [4](#)
- [42] B. Zhou, A. Khosla, A. Lapedriza, A. Oliva, and A. Torralba, "Learning deep features for discriminative localization," in *CVPR*, 2016. [4](#), [5](#), [7](#), [9](#), [10](#), [11](#), [12](#)
- [43] A. Meethal, M. Pedersoli, Z. Zhu, F. Romero, and E. Granger, "Semi-weakly supervised object detection by sampling pseudo ground-truth boxes," in *IJCNN*, 2022. [5](#)

- 
- [44] N. Otsu, “A threshold selection method from gray-level histograms,” *IEEE Transactions on Systems, Man, and Cybernetics*, vol. 9, no. 1, pp. 62–66, 1979. [5](#)
  - [45] C. Wah, S. Branson, W. Steve, P. Peter, and S. Belongie, “The caltech-ucsd birds-200-2011 dataset,” Tech. Rep. CNS-TR-2011-001, California Institute of Technology, 2011. [6](#)
  - [46] J. Deng, W. Dong, R. Socher, L. Li, K. Li, and L. Fei-Fei, “Imagenet: A large-scale hierarchical image database,” in *CVPR*, 2009. [6](#)
  - [47] B. Recht, R. Roelofs, L. Schmidt, and V. Shankar, “Do imagenet classifiers generalize to imagenet?,” in *ICML*, 2019. [7](#)
  - [48] S. Yang, Y. Kim, Y. Kim, and C. Kim, “Combinational class activation maps for weakly supervised object localization,” in *WACV*, 2020. [7](#), [9](#), [10](#), [11](#), [12](#)
  - [49] T. Liu, Z. Yuan, J. Sun, J. Wang, N. Zheng, X. X. Tang, and H. Shum, “Learning to detect a salient object,” *TPAMI*, vol. 33, no. 2, pp. 353–367, 2010. [8](#)